Supporting Materials

Tin Anode for Sodium-Ion Batteries Using Natural Wood Fiber as a Mechanical Buffer and Electrolyte Reservoir

Hongli Zhu,[1 (a)] Zheng Jia,[2 (a)] Yuchen Chen,[1 (a)] Nicholas Weadock,[1] Jiayu Wan,[1] Oeyvind Vaaland,[2] Xiaogang Han,[1] Teng Li,[2*] Liangbing Hu[1*]

Downloaded from pubs.acs.org/naleld/article-supplement/1689112/pdf/nl400998t_si_001/ by YALE UNIV user on 12 September 2026

Electrochemical Performance of Sn film on Cu substrate

The capacity decayed dramatically for the Sn thin film on a stiff Cu substrate. The discharge capacity is 98 mAh/g at the 10th cycle. It has two obvious plateaus at 0.27 V and 0.54 V and two short plateaus at 0.18 V and 0.75 V at the initial cycles. At the 50th cycle, these plateaus are not obvious any more. The discharge specific capacity is only around 22 mAh/g at the 100th cycle.

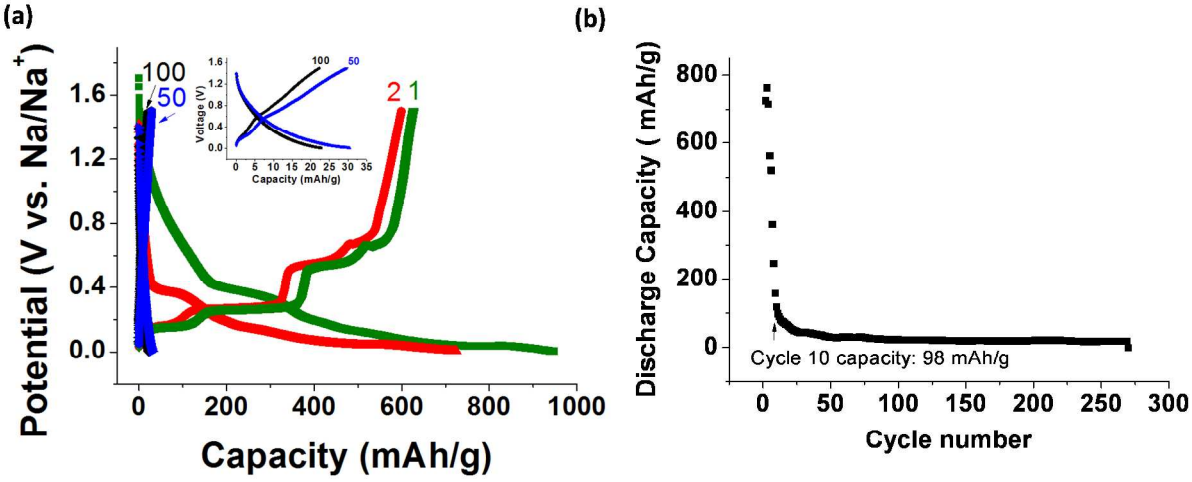


Fig. S1 Electrochemical performance of Sn thin film on hard Cu (a) Voltage profile of the 1st, 2nd , 50th and 100th cycle of Sn nanoparticle thin film on Cu foil at rate C/10 for Na-ion battery. Insert figure is the voltage profile of the 50th and 100th cycle. (b) Cycling performance of Sn thin film on hard Cu.

Methods for Simulation

To gain insights into the wrinkling phenomenon of Sn@WF observed during galvanostatic charge/discharge testing and its role on the better cycling performance of Sn@WF anode, we simulate the sodiation/desodiation (charging/discharging) process and the concurrent mechanical deformation through a fully coupled diffusion-displacement explicit analysis in commercial finite element code ABAQUS 6.10. The Sn film is initially pristine and subjected to a constant sodium flux I_0 at the surface under galvanostatic charging/discharging rate C/10. We employ a constant diffusivity $D = 10^{-14} cm^2/s$ to simulate the sodiation/desodiation process. During the course of charging/discharging, the sodiation state is characterized by how many Na ions are inserted into the tin anode. Here, we define a normalized sodiation state (NSS) as the current sodiation state divided by the maximum sodiation extent observed in the experiment and use it to characterize the charging/discharging state. According to the capacity measured from the experiment, NSS ramps from 0 up to 1 during charging half cycle and finally drops back down to 0 at the end of discharging half cycle. During cycling, Sn film undergoes plastic deformation to accommodate the large volumetric change (about 200%) induced by sodium insertion/extraction. An elastic-perfectly plastic constitutive law with Young's modulus of 40GPa and yielding stress σ_Y of 2GPa is assumed for sodiated Sn. Cellulose fiber is set to be a neo-Hookean material with Young's Modulus of 1.1GPa. Taking advantage of plane strain condition, only the circular cross section of the Sn@WF is simulated in order to reduce the computational cost. The diameter of cellulose fiber and initial thickness of pristine Sn film are $10\mu m$ and 50nm, respectively. The concurrent sodium diffusion and plasticity evolve the

Downloaded from pubs.acs.org/naleld/article-supplement/1689112/pdf/nl400998t_si_001/ by YALE UNIV user on 12 September 2026

wrinkling morphology of cellulose fiber supported Sn film and associated stress distribution.

Details of Simulation and Experimental Results

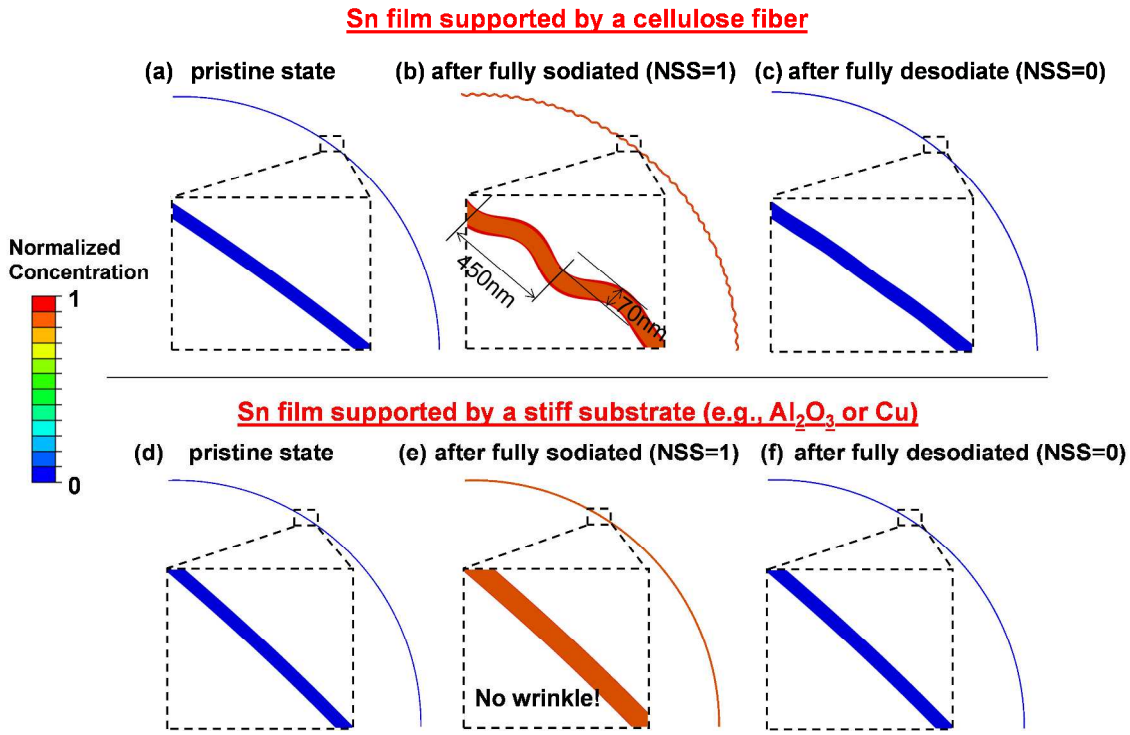


Fig. S2 Morphology evolution of Sn film on a cellulose fiber (a-c) versus that on a stiff substrate (e.g., Al_2O_3 or Cu) (d-f). For clarity, only part of the Sn film is shown here; the fiber and stiff substrate are not shown. (a-c) reveals that Sn@WF wrinkles during charging/discharging cycles. (a) pristine smooth Sn@WF. (b) after fully sodiated, cellulose fiber supported Sn film wrinkles. The wrinkle pattern is characterized by a wavelength of ~450nm and an amplitude of ~70nm. (c) after fully desodiated, wrinkling of the Sn film nearly disappears. (d-f) shows Sn film on a stiff substrate cannot wrinkle. (d) Pristine smooth Sn film on a stiff substrate. After fully sodiated (e)/desodiated (f), the Sn film remains the smooth morphology without wrinkling.

Downloaded from pubs.acs.org/naletd/article-supplement/1689112/pdf/nl400998t_si_001/ by YALE UNIV user on 12 September 2026

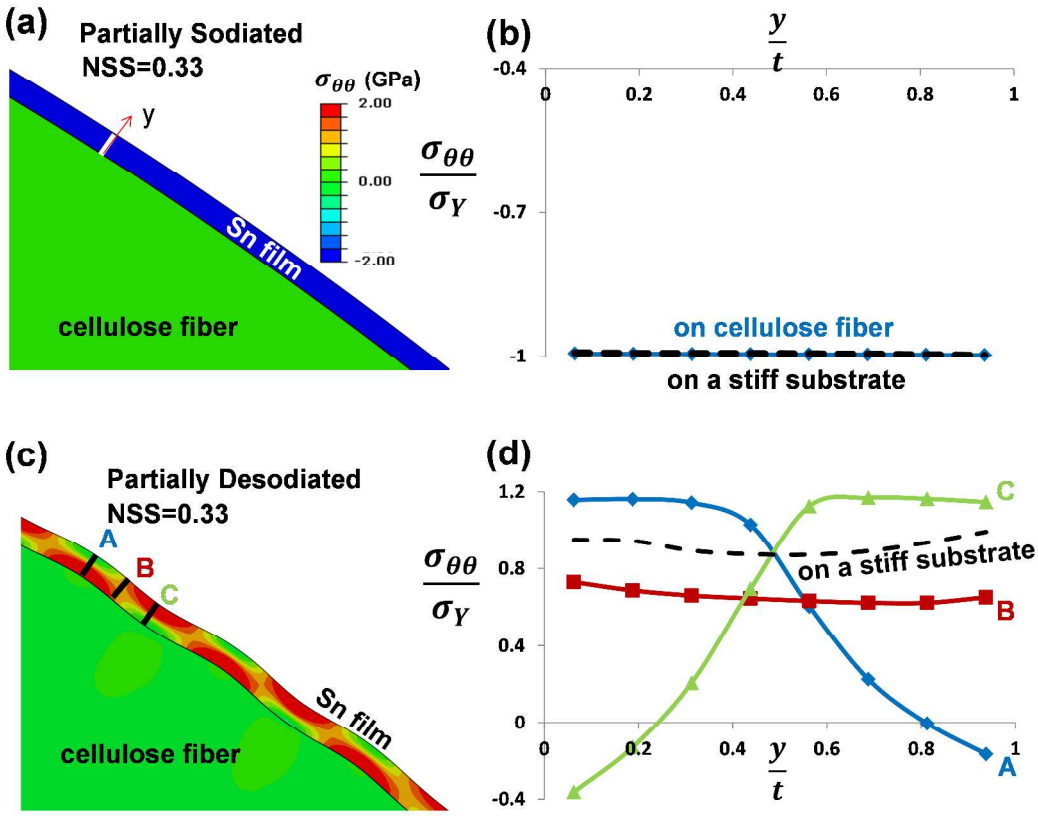


Fig. S3 (a) and (c) show morphology of a 50 nm Sn@WF at intermediate charging and discharging states ($NSS = 0.33$), respectively. Color contours denote the hoop stress ($\sigma_{\theta\theta}$) level. The associated distributions of hoop stress (normalized by yield stress) in the Sn film along thickness direction at three representative locations are plotted in (b) and (d), respectively. For comparison, dark dashed lines in (b) and (d) plot the hoop stress distribution in a Sn film supported by a stiff substrate.

Downloaded from pubs.acs.org/naleifd/article-supplement/1689112/pdf/nl400998t_si_001/ by YALE UNIV user on 12 September 2026

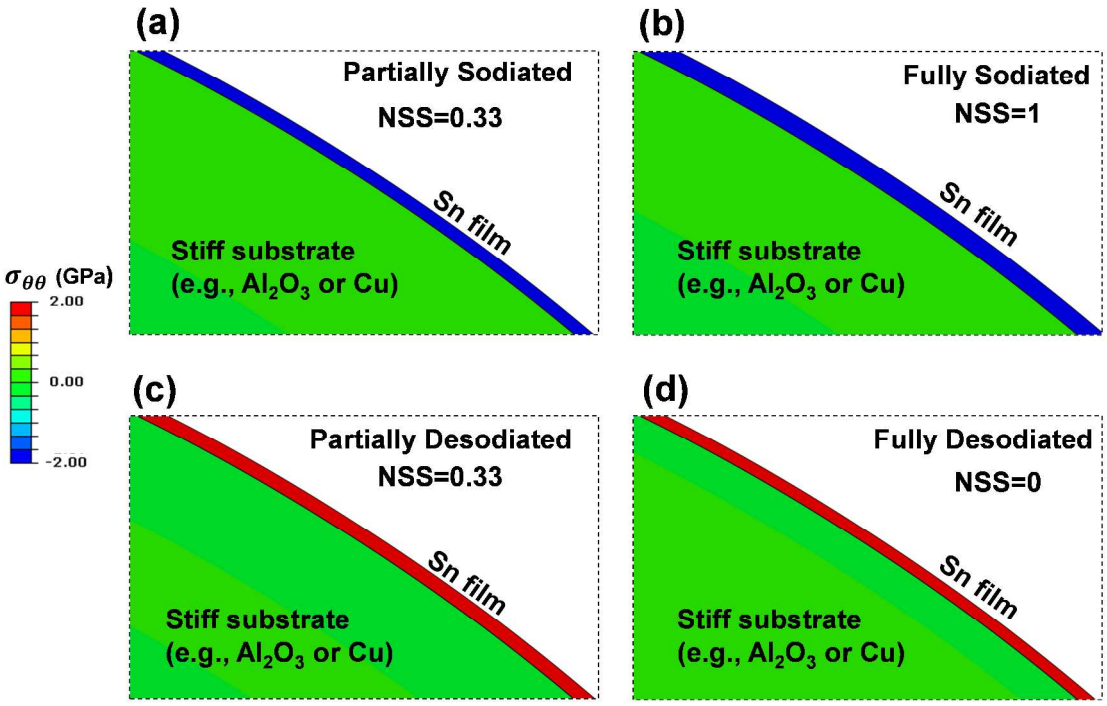


Fig. S4 Hoop stress distribution in stiff substrate supported Sn film during sodiation and desodiation. Hoop stresses in Sn film at (a) intermediate and (b) full sodiation stages are uniform and compressive (~-2GPa), but are tensile (~2GPa) at (c) intermediate and (d) full desodiation stages. Note the smooth morphology and high stress throughout the sodiation/desodiation cycle.

Downloaded from pubs.acs.org/naleld/article-supplement/1689112/pdf/nl400998t_si_001/ by YALE UNIV user on 12 September 2026

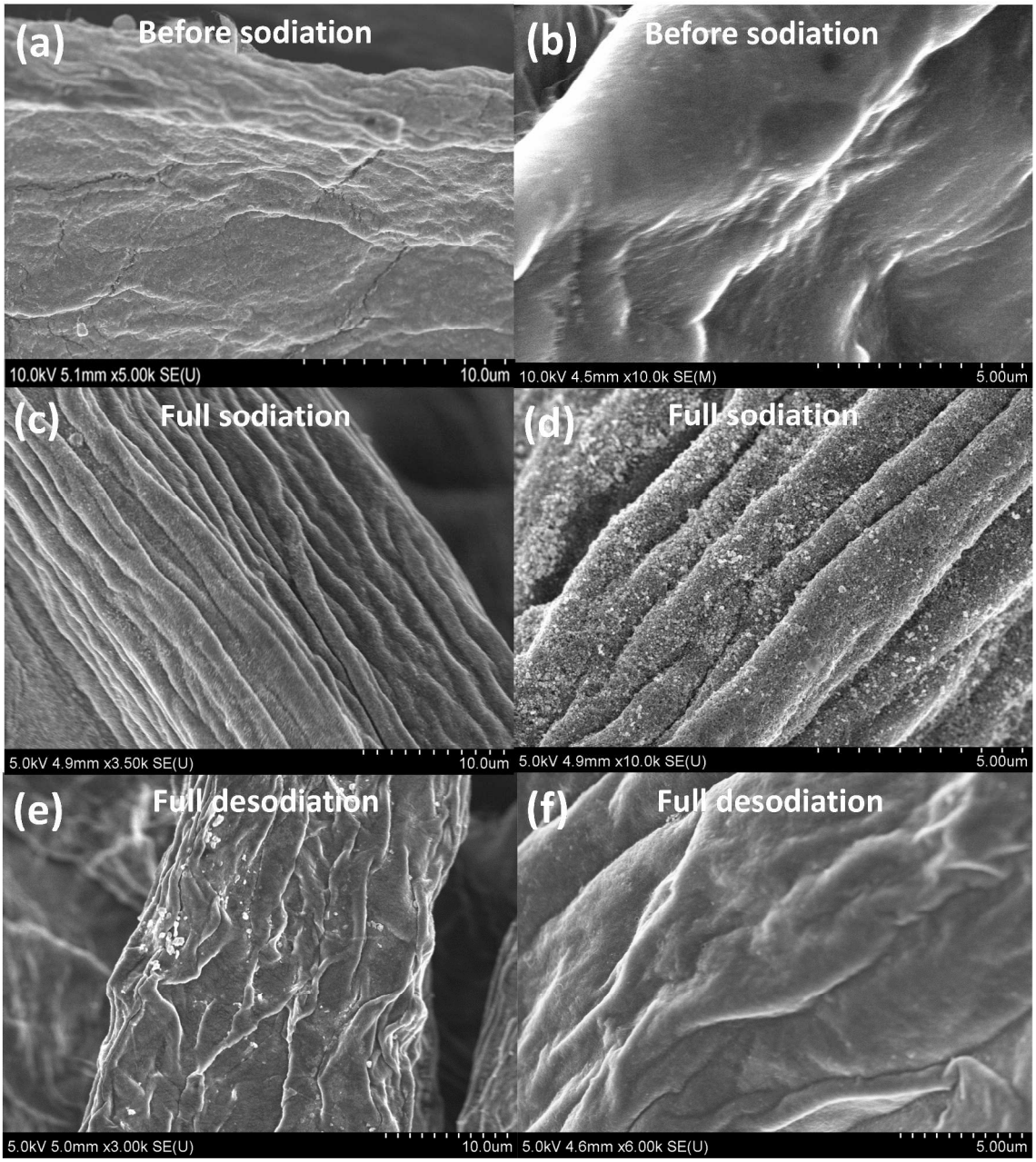


Figure S5: (a), (b) Experimental Scanning Electron Microscope (SEM) images of the morphology of the pristine electrode after electrochemical deposition; (c), (d) Experimental morphology of the fully sodiated electrode after the first half cycle; (e), (f) Morphology of the fully desodiated electrode at the end of the first cycle.

Downloaded from pubs.acs.org/naletd/article-supplement/1689112/pdf/nl400998t_si_001/ by YALE UNIV user on 12 September 2026

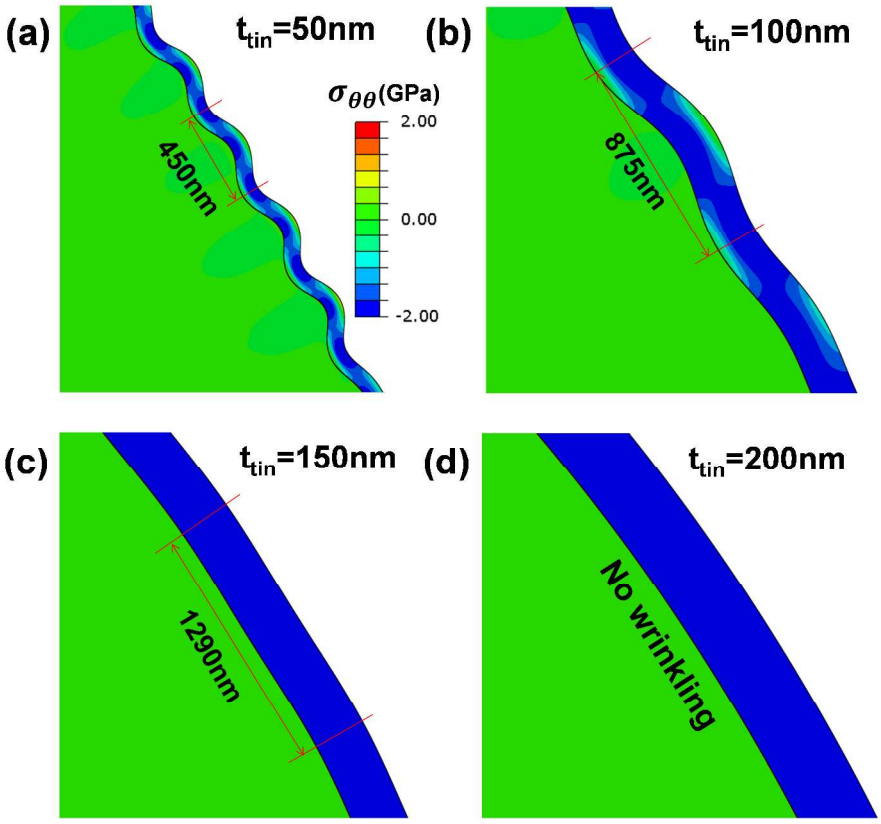


Figure S6. Morphology of cellulose fiber supported tin(Sn) films of various thicknesses (a) t_{tin} = 50nm, (b) 100nm, (c) 150nm, and (d) 200nm at the fully sodiated state. Color contours denote the hoop stress ($\sigma_{\theta\theta}$) level. As t_{tin} increases, the compression-induced wrinkling amplitude decreases and wrinkling wavelength increases. For a 200nm thick Sn film, no wrinkling occurs at full sodiation.

Downloaded from pubs.acs.org/naleifd/article-supplement/1689112/pdf/nl400998t_si_001/ by YALE UNIV user on 12 September 2026

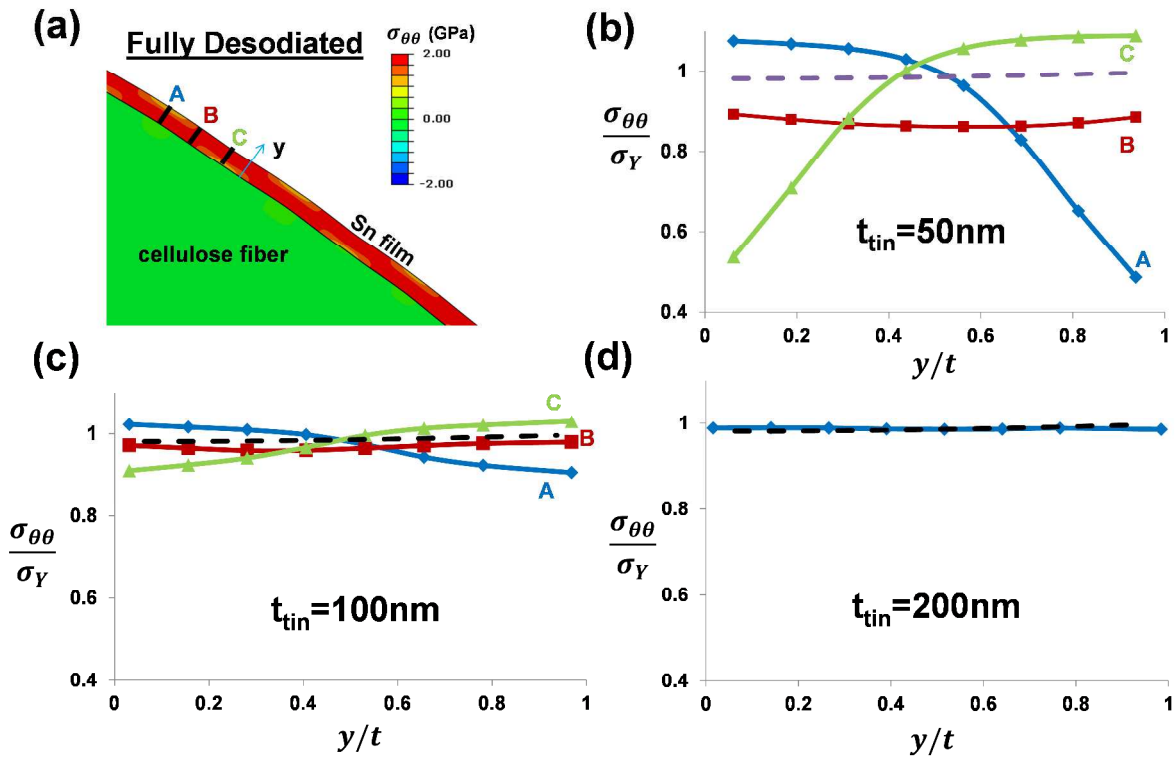


Figure S7. (a) Morphology of a cellulose fiber supported Sn film (50nm thick) at the fully desodiated state. Color contours denote the hoop stress ($\sigma_{\theta\theta}$) level. (b) Plots the associated distributions of hoop stress normalized by yield stress versus location along film thickness. Such distributions of hoop stress in a 100nm-thick and 200-nm thick Sn film are plotted in (c) and (d), respectively. As Sn film thickness increases, wrinkling formation during sodiation diminishes (as shown in Figure S5), which leads to less mitigation of desodiation-induced tensile stress. Without wrinkling (e.g., (d)), the tensile hoop stress is as high as that for an Sn film supported on a stiff substrate (denoted by the dashed line in each plot).

Downloaded from pubs.acs.org/naleld/article-supplement/1689112/pdf/nl400998t_si_001/ by YALE UNIV user on 12 September 2026